

Cluster method for the Hubbard model: local moments and short-range correlations

Arno P. Kampf

Angaben zur Veröffentlichung / Publication details:

Kampf, Arno P. 1991. "Cluster method for the Hubbard model: local moments and short-range correlations." *Physical Review B* 44 (6): 2637–42.
<https://doi.org/10.1103/physrevb.44.2637>.

Nutzungsbedingungen / Terms of use:

licgercopyright

Dieses Dokument wird unter folgenden Bedingungen zur Verfügung gestellt: / This document is made available under the following conditions:

Deutsches Urheberrecht

Weitere Informationen finden Sie unter: / For more information see:

<https://www.uni-augsburg.de/de/organisation/bibliothek/publizieren-zitieren-archivieren/publizieren>



Cluster method for the Hubbard model: Local moments and short-range correlations

A. P. Kampf

Department of Physics, University of California, Santa Barbara, California 93106

(Received 18 March 1991)

We use a functional-integral representation for the Hubbard model to describe the formation of local moments and their magnetic correlations. In the absence of long-range magnetic order, the presence of well-established local moments alone is sufficient to produce a gap in the electronic spectrum. The local moments are treated within a coherent-potential approximation, and we apply an embedded-cluster method to incorporate their interactions.

I. INTRODUCTION

In order to describe the physics of the high- T_c oxide superconductors two alternative approaches have been put forward¹ to account for the magnetic properties and the proximity in the phase diagram of antiferromagnetism and superconductivity. In strong-coupling theories the on-site Coulomb repulsion between the carriers is assumed to be large compared to their effective bandwidth allowing to project onto the Hilbert space with no double occupancy of sites. Within an effective one-band model this gives rise to t - J or t - t' - J models describing the correlated hopping of holes in the background of antiferromagnetically coupled spins. While these approaches should be correct for the lightly doped compounds, a description in terms of itinerant electrons may be more appropriate in the intermediate doping regime of the superconducting compounds. Alternatively, in weak-coupling theories antiferromagnetism arises from the formation of a spin-density wave (SDW).² The long-range spin order of the SDW leads to a gap in the single-particle excitation spectrum. Hole doping destroys the long-range order, but finite-range spin correlations still give rise to a pseudogap in the density of states.³ Since the cuprates may very well be in an intermediate-coupling regime with a Coulomb repulsion comparable to the bandwidth,⁴ either approach is valid as a starting point to discuss the novel properties of the cuprates.

A weak-coupling SDW approach, however, does not properly include the presence of local moments. The long-range order of the SDW at zero temperature and half-filling can be destroyed either by doping with holes or electrons or by increasing the temperature above the Néel temperature T_N . The true SDW gap in the single-particle spectrum is then reduced to a pseudogap with a finite density of states at the Fermi level. The system therefore is no longer an insulator but a conductor. The antiferromagnetic parent compounds, however, are still insulating due to a Mott-Hubbard gap even above their Néel temperature where the magnetic order is only short range. It is well known that the presence of the well-established local moments alone is responsible for the insulating behavior⁵ and it is important to incorporate their presence in any theoretical description.

Earlier attempts to understand the local-moment formation in the framework of the single-band Hubbard

model have used the static approximation within the Hubbard-Stratonovich functional integral scheme. In this scheme the paramagnetic phase is considered as a disordered alloy of up and down magnetic moments.^{5,6} A disordered alloy is known to have a gap in the density of states if the difference between the atomic levels is larger than the bandwidth and this analogy leads to the insulating behavior of the disordered local-moment regime.

In this paper we will take a similar line of arguments, but we will apply a more sophisticated cluster-alloy theory,⁷ which was developed in recent years to account for short-range correlations beyond the single-site approximation of the commonly used coherent potential approximation (CPA). In fact, we will start with the CPA to describe an effective medium in which we embed a cluster of sites where local correlations of the moments are treated by weighted configurational averages. The method is described in Secs. II and III. Small cluster results for a half-filled band are presented in Sec. IV. The inclusion of fluctuations is discussed in Sec. V, giving an outlook of how the present method can be extended to investigate fluctuating local moments with short-range correlations.

II. FUNCTIONAL INTEGRAL SCHEME: CPA

We consider an effective single-band Hubbard model on a square lattice

$$H = \sum_{\mathbf{k}, \sigma} \varepsilon_{\mathbf{k}} c_{\mathbf{k}\sigma}^\dagger c_{\mathbf{k}\sigma} + U \sum_i n_{i\uparrow} n_{i\downarrow} - \mu N_e, \quad (1)$$

with the tight binding dispersion $\varepsilon(\mathbf{k}) = -2t[\cos(k_x a) + \cos(k_y a)]$ and the chemical potential μ for N_e electrons. U is the intra-atomic electron-electron interaction and t is the nearest-neighbor hopping integral. The Hubbard interaction can be rewritten in several ways leading to some ambiguities in the functional integral method.⁸ In the present paper we will apply the two-field method which starts from

$$U n_{i\uparrow} n_{i\downarrow} = \frac{U}{4} (n_{i\uparrow} + n_{i\downarrow})^2 - \frac{U}{4} (n_{i\uparrow} - n_{i\downarrow})^2 \quad (2)$$

and has the advantage that its saddle-point approximation (SPA) yields the Hartree-Fock theory, although the SPA breaks the rotational invariance for the magnetic moments.⁹ After the Hubbard-Stratonovich (HS) decoupling the partition function in this scheme is given by

$$Z = \int \prod_i \mathcal{D}x_i(\tau) \int \prod_j \mathcal{D}y_j(\tau) \exp \left[-\pi \int_0^1 \sum_l [x_l^2(\tau') + y_l^2(\tau')] d\tau' \right] Z[x, y], \quad (3a)$$

$$Z[x, y] = \text{Tr} T \exp \left[-\int_0^1 \left[\beta \sum_{\mathbf{k}\sigma} (\epsilon_{\mathbf{k}} - \mu) c_{\mathbf{k}\sigma}^\dagger c_{\mathbf{k}\sigma} + \sum_{i\sigma} v_{i\sigma}(\tau') n_{i\sigma}(\tau') \right] d\tau' \right], \quad (3b)$$

$$v_{i\sigma}(\tau) = \sqrt{\pi\beta U} [\sigma x_i(\tau) + iy_i(\tau)]. \quad (3c)$$

The many-electron problem of the Hubbard model is thus transformed into a complicated one-electron problem in a complex and time-dependent potential and a functional integration over the potential itself. In the static approximation all time dependences are neglected, which is supposed to be a good approximation when the flipping time $\hbar U/t^2$ of a magnetic moment is long compared to the electronic hopping time $\hbar t^{-1}$, i.e., for U/t large.⁵ In this limit charge fluctuations are negligible and the y field, which decouples the charge component of the interaction Eq. (2), is replaced by its saddle-point value y^0

$$\sqrt{\pi U/\beta} y_j^0 = i \frac{U}{2} \langle n_{j\uparrow} + n_{j\downarrow} \rangle, \quad (4a)$$

while the saddle point for the x field determines the magnitude of the local moment

$$\Delta_i^0 = \sqrt{\pi U/\beta} x_i^0 = \frac{U}{2} \langle n_{i\uparrow} - n_{i\downarrow} \rangle. \quad (4b)$$

In the above approximations the functional integral reduces to a simple integral over all values of the local magnetic moments. The trace over the fermion fields is therefore reduced to an alloy problem with diagonal disorder and with the magnetic potentials $-\Delta_i$ on the sites.¹⁰ The probability for a given distribution of the Δ_i 's is $e^{-\beta \mathcal{F}(\Delta_1, \dots, \Delta_N)}$, where

$$\begin{aligned} & -\beta \mathcal{F}(\Delta_1, \dots, \Delta_N) \\ &= -\sum_i \frac{\beta \Delta_i^2}{U} + \sum_{i\sigma} \int_{-\infty}^{+\infty} \rho_{i\sigma}(\Delta_1, \dots, \Delta_N; \omega) \\ & \quad \times \ln(1 + e^{-\beta(\omega - \mu)}) d\omega, \end{aligned} \quad (5)$$

$\rho_{i\sigma}$ is the local density of states on site i , and N is the number of sites. The total free energy F is then to be determined from

$$\begin{aligned} Z &= e^{-\beta F} = e^{-(\beta U/4) \langle n_{i\uparrow} + n_{i\downarrow} \rangle N} \\ & \quad \times \int \prod_{i=1}^N d\Delta_i e^{-\beta \mathcal{F}(\Delta_1, \dots, \Delta_N)}. \end{aligned} \quad (6)$$

It is well known¹¹ that there are two symmetric minima for $\mathcal{F}(\Delta)$ when Δ_i^0 is different from zero. In the paramagnetic regime we start by neglecting the short-range correlations between the local moments and assume that $\rho_{i\sigma}$ depends on the local value of Δ_i only. $\rho_{i\sigma}$ is then calculated in the coherent potential approximation¹² for a random binary alloy of potentials $\pm|\Delta|$:

$$\rho_{i\sigma}(\omega - \mu) = \frac{1}{\pi} \text{Im} \frac{G_{ii}^0[\omega - \Sigma(\omega)]}{1 - [\Delta_i - \Sigma(\omega)] G_{ii}^0[\omega - \Sigma(\omega)]}. \quad (7)$$

G_{ii}^0 is the local Green's function of the unperturbed tight-binding band

$$G_{ii}^0(\omega) = \frac{1}{N} \sum_{\mathbf{k}} \frac{1}{\omega - (\epsilon_{\mathbf{k}} - \mu)} = \frac{2}{\pi(\omega + \mu)} K \left[\frac{4t}{\omega + \mu} \right], \quad (8)$$

where K is the complete elliptic integral of the first kind. The CPA site-diagonal self-energy $\Sigma(\omega)$ is determined by the condition⁶

$$\Sigma(z) = [\Delta^2 - \Sigma^2(z)] G_{ii}^0[z - \Sigma(z)]. \quad (9)$$

In Fig. 1 we plot, as in Ref. 8, the local density of states for different values of the effective potential Δ for the case of one electron per site with $\mu=0$. For small Δ/t the band is broadened slightly and the van Hove singularity at the band center is suppressed. As expected, for values of Δ larger than half of the bandwidth of the noninteracting tight-binding band $\Delta > 2t$ a gap develops around $\omega = \mu = 0$. With decreasing temperature the corresponding free energy as calculated from Eq. (5) develops a local minimum as a function of Δ , which further shifts to larger values of Δ when the temperature is lowered. Since Δ is by Eq. (4b) directly related to the magnitude of the local moment, the system becomes more magnetic with decreasing temperature.

III. CLUSTER METHOD

Although the CPA treatment has the appealing feature that it describes the formation of local magnetic moments and the appearance of the Mott-Hubbard gap in a simple way, any sort of magnetic ordering is already beyond the scope of this single-site treatment, since no interaction between the moments is taken into account. The short-range correlations, however, can be incorporated by using the embedded-cluster method (ECM) (Ref. 7) method from alloy theory that was originally invented to study the effects of local clustering of atoms on the electronic properties of the alloy. In the language of the Hubbard model this precisely corresponds to local magnetic ordering. The embedded cluster method is in detail described in the literature,^{7,13} but for the sake of completeness we will in the following outline the basics of its computational procedure.

In the static approximation the HS decoupling leads to a tight-binding Hamiltonian for electrons on a lattice with diagonal disorder

$$H = \sum_{i,\sigma} v_{i,\sigma} c_{i\sigma}^\dagger c_{i\sigma} + \sum_{ij,\sigma} t_{ij} c_{i\sigma}^\dagger c_{j\sigma}, \quad (10)$$

where the local potentials $v_{i,\sigma}$ are given by the auxiliary

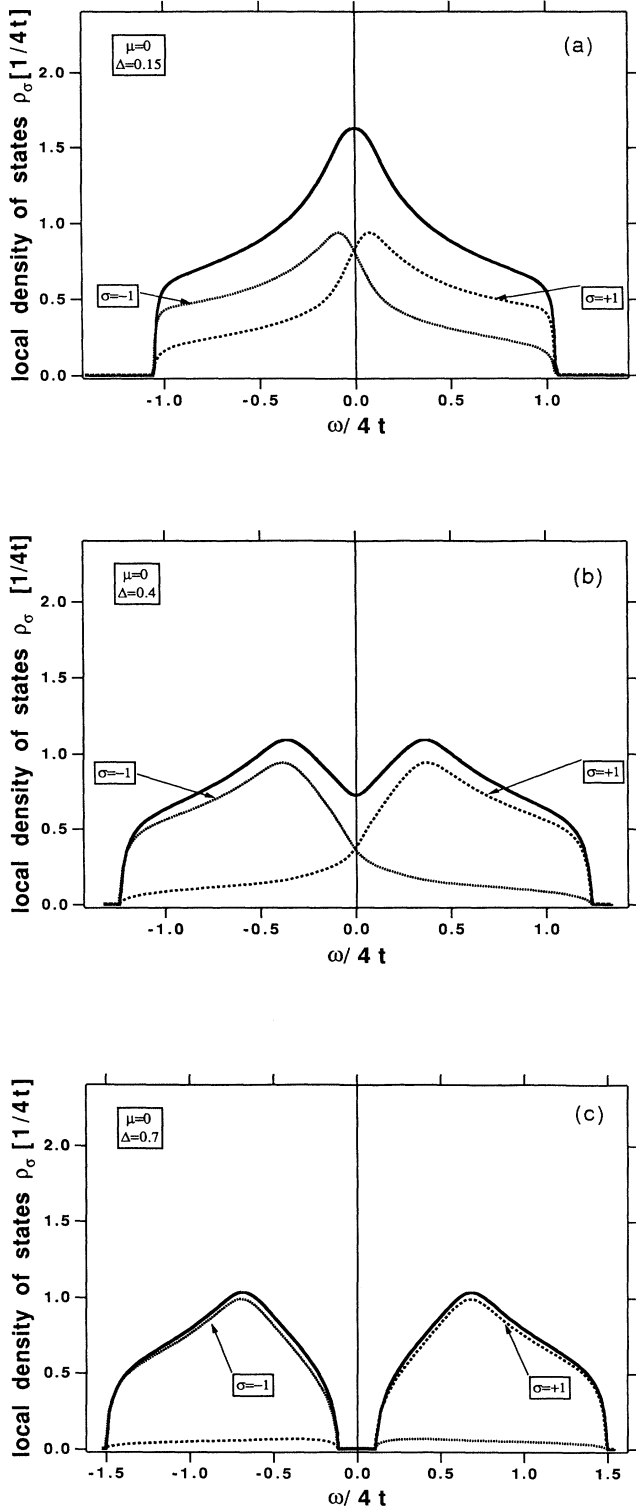


FIG. 1. Local density of states for a random binary alloy with local potentials $\pm\Delta$ based on a two-dimensional tight binding band. (a) $|\Delta|=0.15$, (b) $|\Delta|=0.40$, and (c) $|\Delta|=0.70$. Dashed lines correspond to the case where the local potential at the given site is $\sigma|\Delta|$ with $\sigma=\pm$ and their sum is given by the continuous line. Energies are measured in units of $4t$.

HS fields. The Dyson equation for the single-particle Green's function is now split up into the contributions from lattice sites inside and outside of an arbitrarily chosen cluster \mathcal{C}

$$G_{ij,\sigma} = g_{i,\sigma} \left[\delta_{ij} + \sum_{k \in \mathcal{C}} t_{ij} G_{kj,\sigma} + \sum_{k \notin \mathcal{C}} t_{ik} G_{kj,\sigma} \right]. \quad (11)$$

$g_{i,\sigma}(z) = [z - (v_{i,\sigma} - \mu)]^{-1}$ is the bare local Green's function in the absence of hopping. For $i, j \in \mathcal{C}$ the last term in the Dyson equation can formally be treated as a perturbation and Eq. (11) is iteratively solved by introducing a matrix $\Delta_{ik}^{\mathcal{C}}$

$$\sum_{k \notin \mathcal{C}} t_{ik} G_{kj,\sigma} = \sum_{k \in \mathcal{C}} \Delta_{ik}^{\mathcal{C}} G_{kj,\sigma} \quad (12)$$

for $i \in \mathcal{C}$. The matrix Δ represents the sum of all hopping paths that start and end at sites inside the cluster but avoid all cluster sites at intermediate steps:

$$\Delta_{ik}^{\mathcal{C}} = \sum_{n \notin \mathcal{C}} t_{in} g_n t_{nk} + \sum_{n, m \notin \mathcal{C}} t_{in} g_n t_{nm} g_m t_{mk} + \dots \quad (13)$$

With the matrix $\Delta^{\mathcal{C}}$ we easily solve for G inside the cluster. The key idea of the method now is to recognize that $\Delta^{\mathcal{C}}$ depends only on the part of the system outside the cluster, but it is independent of the configuration inside the cluster. We will therefore assume that the cluster is surrounded by an effective medium that we describe within the coherent potential approximation, i.e., the local Green's function outside the cluster is given by

$$g_{i,\sigma}^{\text{CPA}}(z) = \frac{1}{z - [\Sigma(z) - \mu]} \quad (14)$$

and independent of the site. Using the local CPA Green's function in the expansion for $\Delta^{\mathcal{C}}$, the intracluster Green's function matrix is given by

$$\underline{G}^{\mathcal{C}}(z) = [z \mathbf{1} - \underline{H} - \Delta_{\text{CPA}}^{\mathcal{C}}]^{-1}, \quad (15)$$

where the matrix elements of \underline{H} are defined by

$$H_{ij} = \begin{cases} v_{i,\sigma} & \text{if } i=j \\ t_{ij} & \text{if } i \neq j. \end{cases} \quad (16)$$

If we disregard the distinction between sites inside and outside the cluster and treat the whole system within CPA, we know that

$$(\underline{G}_{\text{CPA}}^{\mathcal{C}})_{ij} = \frac{1}{N} \sum_{\mathbf{k}} \frac{e^{i\mathbf{k}(\mathbf{R}_i - \mathbf{R}_j)}}{z - (\epsilon_{\mathbf{k}} - \mu) - \Sigma(z)}. \quad (17)$$

This in turn can be used to determine the matrix $\Delta_{\text{CPA}}^{\mathcal{C}}$ in Eq. (15) and we finally obtain

$$\underline{G}^{\mathcal{C}}(z) = [\bar{\underline{H}} - \underline{H} + \underline{G}_{\text{CPA}}^{-1}(z)]^{-1}. \quad (18)$$

The matrix elements of $\bar{\underline{H}}$ differ from those of \underline{H} in that the local potentials $v_{i,\sigma}$ are replaced by the CPA self-energy $\Sigma(z)$.

Inside the cluster it is now possible to perform a weighted average over the static auxiliary HS fields. The weight factor is determined by the free energy Eq. (5) of a given configuration. The advantage of the cluster method is that for a small enough cluster we can indeed

perform the configurational average and the magnetic correlations between the local magnetic moments manifest themselves by the lower free energy of specific “up” and “down” arrangements of the moments. For obvious reasons we will choose a highly symmetric cluster of sites and in particular be interested in the local density of states $\rho_i^{\mathcal{E}} = -1/\pi \text{Im}G_{ii}^{\mathcal{E}}$ at the center of the cluster.

IV. NUMERICAL CALCULATIONS

For an illustration of the method we will in the following present the calculations for the smallest meaningful cluster: a star-shaped five-site cluster for the two-dimensional square lattice. Given the CPA self-energy and a specific configuration of local potentials Δ , i.e., local moments, the calculation of $\underline{G}^{\mathcal{E}}$ is simple and involves only the inversion of complex matrices of dimension $N_c \times N_c$, where N_c is the number of sites inside the cluster. In addition, the lattice Green’s functions¹⁴

$$G_{ij}^0(z) = \frac{1}{N} \sum_{\mathbf{k}} \frac{e^{i\mathbf{k} \cdot \mathbf{R}_{ij}}}{z - (\epsilon_{\mathbf{k}} - \mu)} \quad (19)$$

have to be evaluated for arbitrary complex arguments and sites $i, j \in \mathcal{E}$.

As for the CPA calculation in Sec. II we also adopt the binary alloy approximation for the calculation of the cluster Green’s function, i.e., we consider all possible 2^5 configurations of potentials $\pm|\Delta|$ on the five cluster sites. But due to their degeneracy, actually only the six arrangements shown in Fig. 2 need to be evaluated. For each configuration \mathcal{A} the corresponding contribution from the central cluster site to the free energy is calculated from Eq. (5). The relative weight of a given configuration \mathcal{A} is then determined by

$$P_{\mathcal{A}} = \frac{e^{-\beta \mathcal{F}[\Delta_1, \dots, \Delta_{N_c}]}}{\sum_{i=1, \dots, 2^{N_c}} e^{-\beta \mathcal{F}_{\mathcal{A}_i}}}. \quad (20)$$

Figure 3 shows the local density of states at the cluster

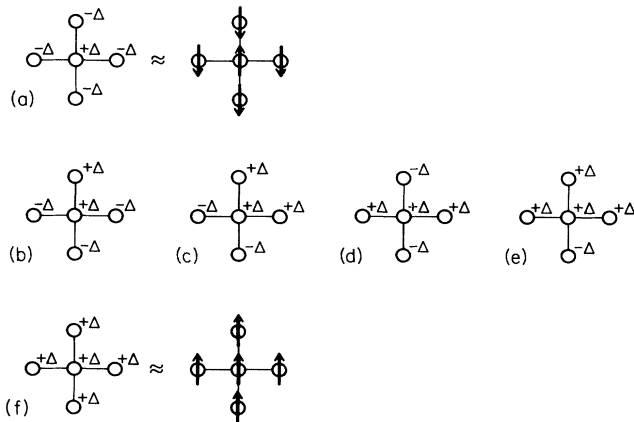


FIG. 2. Configurations of local potentials $\pm\Delta$, i.e., “up” and “down” magnetic moments for the five-site cluster for a fixed potential $+\Delta$ at the center. (a) is an antiferromagnetic and (f) a ferromagnetic arrangement.

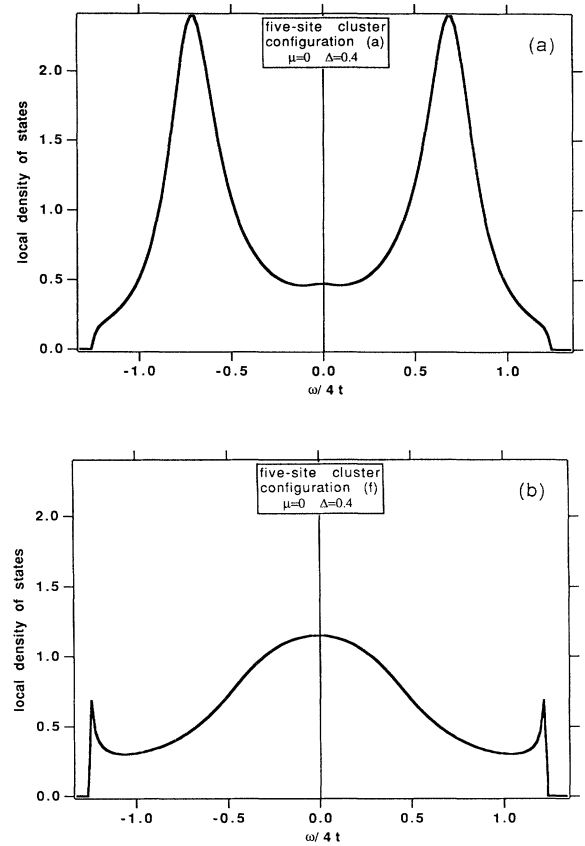


FIG. 3. Local density of states at the center of the five-site cluster calculated by the embedded-cluster method (a) for the antiferromagnetic and (b) for the ferromagnetic configuration.

center for the totally antiferromagnetic and ferromagnetic configurations. A value of Δ was chosen for which the CPA calculation in Sec. II did not develop a gap in the density of states, but only a pseudogap (see Fig. 1). The “ferromagnetic” configuration shows an enhancement around $\omega = \mu = 0$, while the “antiferromagnetic” configuration further deepens the pseudogap, indicating the expected tendency towards the formation of a true gap with antiferromagnetic spin order.¹⁵ Most remarkable, however, are the differences in the cluster free energies of the different configurations as listed in Table I. For the chosen parameters, temperature, and U/t , the antiferromagnetic configuration has by far the lowest free energy \mathcal{F} and translated into a relative weight according to Eq. (20) any other configuration contributes less than 6% to the partition function. The configurationally averaged local density of states is therefore barely distinguishable from the density of states shown in Fig. 3(a) for the antiferromagnetic configuration. The above numbers do of course depend on U/t and the temperature, but presumably not very sensitively on the cluster size as calculations on a nine-site cluster did indeed indicate. The embedded-cluster method therefore in a very simple way nicely demonstrates how the many-body correlations, i.e., the magnetic ordering, are reinstated by the functional integration over all the single-particle alloy problems by

TABLE I. Parameters chosen for the five-site cluster calculation: $|\Delta|=1.6t$, $T=0.2t$, and $U=4t$.

Configuration \mathcal{A}	Free energy $\mathcal{F}/4t$	Probability $P_{\mathcal{A}}$
(a)	-0.562	0.9422
(b)	-0.340	0.0110
(c)	-0.246	0.0017
(d)	-0.260	0.0022
(e)	-0.175	0.0004
(f)	-0.226	0.0011

its selection of the relevant static configurations (or dynamic paths beyond the static approximation).

V. EXTENSIONS: SUMMARY

There are several ways to improve on the method outlined so far. First we can improve on the treatment of the cluster environment by including small fluctuations of the HS potentials $\Delta_i(\tau)$ around their saddle-point values. The corrections to the CPA formulation are then most naturally incorporated by rewriting the trace over the time evolution operator $Z[x]$ Eq. (3b) for the time-dependent alloy problem as¹¹

$$Z[x] = e^{\text{Tr} \ln(\underline{G}_0 \underline{G}^{-1})}, \quad (21)$$

again keeping the y field fixed to its saddle-point value. \underline{G} is the exact single-particle propagator of the alloy problem and \underline{G}_0 is the propagator in the absence of interactions

$$G_0^{ij,\sigma}(i\omega_\nu) = \frac{1}{N} \sum_{\mathbf{k}} \frac{e^{i\mathbf{k}\cdot\mathbf{R}_{ij}}}{i\omega_\nu - (\epsilon_{\mathbf{k}} - \mu)}. \quad (22)$$

The trace has to be performed with respect to the site indices i , σ , and ν , where ν labels the fermionic Matsubara frequencies $\omega_\nu = (2n+1)\pi/\beta$. Since we want to keep the CPA propagator as a leading approximation, we write

$$\begin{aligned} \ln(Z[x]) &= \text{Tr} \ln(\underline{G}_0 \underline{G}_{\text{CPA}}^{-1}) \\ &+ \text{Tr} \ln[1 + \underline{G}_{\text{CPA}}(\underline{G}^{-1} - \underline{G}_{\text{CPA}}^{-1})] \end{aligned} \quad (23)$$

and expand the last logarithm to second order in $(\underline{\Sigma}_{\text{CPA}} - \nu)$, where ν is the alloy potential Eq. (3c). This expansion leads to

$$\begin{aligned} \ln(Z[x]) &= \text{Tr} \ln(1 - \underline{\Sigma}_{\text{CPA}} \underline{G}_0) + \text{Tr}(\underline{G}_{\text{CPA}} \underline{\Sigma}_{\text{CPA}}) \\ &+ \beta \sum_{\mathbf{q}, n} |\Delta(\mathbf{q}, i\omega_n)|^2 \Phi_{\text{CPA}}^0(\mathbf{q}, i\omega_n) \\ &- \frac{1}{2} \text{Tr}(\underline{\Sigma}_{\text{CPA}} \underline{G}_{\text{CPA}} \underline{\Sigma}_{\text{CPA}} \underline{G}_{\text{CPA}}). \end{aligned} \quad (24)$$

In analogy to the ‘‘polarization bubble’’ of the noninteracting case we have defined the CPA bubble $\Phi_{\text{CPA}}^0(\mathbf{q}, i\omega_n)$ by

$$\begin{aligned} \Phi_{\text{CPA}}^0(\mathbf{q}, i\omega_n) &= -\frac{1}{\beta} \sum_{\mathbf{k}, \mu} G_{\text{CPA}}(\mathbf{k} + \mathbf{q}, i\omega_\mu + i\omega_n) \\ &\times G_{\text{CPA}}(\mathbf{k}, i\omega_\mu) \end{aligned} \quad (25)$$

for the bosonic Matsubara frequencies $\omega_n = 2\pi n/\beta$. Since the dynamic spin susceptibility is directly related to the mean-square fluctuations of the auxiliary field $\Delta_i(\tau)$ by¹⁶

$$\chi(\mathbf{q}, i\omega_n) = \frac{1}{U} \left[\frac{2\beta}{U} \langle |\Delta(\mathbf{q}, i\omega_n)|^2 \rangle - 1 \right], \quad (26)$$

the functional integration immediately leads to a random-phase-approximation-like result for $\chi(\mathbf{q}, i\omega_n)$

$$\chi(\mathbf{q}, i\omega_n) = \frac{\Phi_{\text{CPA}}^0(\mathbf{q}, i\omega_n)}{1 - U \Phi_{\text{CPA}}^0(\mathbf{q}, i\omega_n)}. \quad (27)$$

This result holds for finite frequencies $i\omega_n \neq 0$. For $i\omega_n = 0$ the dependence of the CPA self-energy on the static alloy configurations has to be taken into account. However, as long as the (imaginary) time-averaged part of the auxiliary field is assumed to be fixed to the saddle-point value, the static susceptibility is determined by the saddle-point alone. The form Eq. (26) for the susceptibility is interesting in itself and it is currently investigated independently from the cluster method.¹⁷

The second line of extensions addresses the treatment of the cluster itself, in particular, the question how fluctuations of the auxiliary fields can be incorporated. Within an adiabatic approximation it is in fact straightforward to include a time dependence of the fields or, equivalently, the local moment parameters $\Delta_i(\tau)$. In this approximation the intracluster Green’s-function matrix \underline{G}^e is calculated for the ‘‘snapshot’’ configurations of the auxiliary fields at a given time τ . Standard available Monte Carlo algorithms can be used to perform the functional integral by sampling over the fields inside the cluster. This procedure, in the adiabatic approximation, would allow to describe fluctuating local moments with short-range correlations inside the small cluster, yet the infinite system is represented by the CPA self-energy for the effective medium surrounding the cluster. It will be interesting to compare the ECM cluster results with quantum Monte Carlo data obtained on finite lattices of the same size. Numerical calculations in this direction are already in preparation and their results will be reported elsewhere.

ACKNOWLEDGMENTS

The author is grateful to K. Bedell, M. Boring, W. Brenig, D. Coffey, and J. R. Schrieffer for helpful conversations. Part of this work was performed within the Advanced Studies Program in High Temperature Superconductivity Theory hosted by the Center for Materials Science at the Los Alamos National Laboratory. This work was also supported in part by the National Science Foundation under Grant No. DMR-89-18307 and by Electric Power Research Institute Grant No. RP 8009-18.

- ¹For a review, see P. A. Lee, in *Proceedings on High Temperature Superconductivity: The Los Alamos Symposium 1989*, edited by K. S. Bedell, D. Coffey, D. E. Meltzer, D. Pines, and J. R. Schrieffer (Addison Wesley, Redwood City, CA, 1990).
- ²J. R. Schrieffer, X. G. Wen, and S. C. Zhang, *Phys. Rev. B* **39**, 11 663 (1989).
- ³A. P. Kampf and J. R. Schrieffer, *Phys. Rev. B* **41**, 6399 (1990).
- ⁴For a discussion of this issue, see J. Friedel (unpublished); and J. Friedel, *J. Phys. Condens. Matter* **1**, 7757 (1989).
- ⁵P. Lacour-Gayet and M. Cyrot, *J. Phys. C* **7**, 400 (1974); M. Cyrot, *J. Phys. (Paris)* **33**, 125 (1972); *Philos. Mag.* **25**, 1031 (1972).
- ⁶J. C. Kimball and J. R. Schrieffer (unpublished).
- ⁷A. Gonis and A. J. Freeman, *Phys. Rev. B* **29**, 4277 (1984).
- ⁸R. F. Hasing and D. M. Esterling, *Phys. Rev. B* **7**, 432 (1972).
- ⁹J. Hubbard, *Phys. Rev. B* **19**, 2626 (1979).
- ¹⁰M. Cyrot, *Phys. Rev. Lett.* **25**, 871 (1970).
- ¹¹J. R. Schrieffer (unpublished).
- ¹²P. Soven, *Phys. Rev.* **156**, 809 (1967); **178**, 1136 (1969); B. Velicky, S. Kirkpatrick, and H. Ehrenreich, *ibid.* **175**, 747 (1969).
- ¹³A. Gonis and J. W. Garland, *Phys. Rev. B* **16**, 2424 (1977); **18**, 3999 (1978); D. J. Whitelaw, *J. Phys. C* **14**, 2871 (1981).
- ¹⁴T. Morita, *J. Math. Phys.* **12**, 1744 (1971); S. Katsura, T. Morita, S. Inawashiro, T. Horiguchi, and Y. Abe, *ibid.* **12**, 892 (1971).
- ¹⁵A. P. Kampf and J. R. Schrieffer, *Phys. Rev. B* **42**, 7976 (1990).
- ¹⁶S. Q. Wang, W. E. Evenson, and J. R. Schrieffer, *Phys. Rev. Lett.* **23**, 92 (1969).
- ¹⁷A. P. Kampf (unpublished).